ROYAL SOCIETY
OF CHEMISTRY

PAPER

Check for updates

Ternifolipyrons A–J: new cytotoxic α-pyrones from *Isodon ternifolius* (D. Don) Kudô†

Abdelsamed I. Elshamy, [ID] *[a] Tarik A. Mohamed, [ID] [b] Ningombam Swapana,[cd] Yusuke Kasai,[c] Masaaki Noji,[c] Thomas Efferth,[e] Hiroshi Imagawa,[c] Mohamed-Elamir F. Hegazy*[be] and Akemi Umeyama [ID] *[c]

Isodon ternifolius (D.Don) Kudô is an important Asian herb used in traditional medicine against several diseases. Nineteen compounds were isolated from the dichloromethane–methanol (1 : 1) extract of *I. ternifolius* roots, including ten new α-pyrone derivatives, named ternifolipyrons A–J. The chemical structures of the isolates were determined by a combination of 1D and 2D NMR, along with LR- and HRMS spectroscopy. The absolute configurations of the α-pyrone derivatives were constructed based upon the X-ray signal crystal of the bromobenzoyl derivative of **1** as well as the electronic circular dichroism (ECD). All isolates (**1–19**) were investigated for their growth-inhibitory potential towards CCRF-CEM-leukemia cells at a fixed concentration of 30 μM. The compounds which exerted more than 50% inhibition at this concentration, compounds (**7**, **10**, **12**, **15–17**), were tested at a different concentration range to determine their IC_{50} values in CCRF-CEM leukemia, MDA-MB-231 triple-negative breast cancer, and MCF7 breast cancer cell lines. Ursolic acid (**16**) showed the most potent activity against the three cancer cell lines with IC_{50} values of 8.37, 18.04, and 18.93 μM, respectively.

1. Introduction

The ≈150 species belonging to the *Isodon* genus are common in tropical and subtropical Asian areas.[1] In traditional medicines, several *Isodon* species were medicinally used for the treatment of many microbial diseases, infections in the gastrointestinal and respiratory systems, tumors, inflammation, and hypertension.[1–3] Recently, numerous clinical trial studies revealed the medicinal significance of these plants such as their anti-inflammatory, antimalarial, anti-enteritis, anti-jaundice, hepatoprotective effects; as well as the treatment of gastrointestinal ailments, arthralgia, hepatitis, and mastitis.[1,2,4] Chemically, the *Isodon* species were documented to synthesize diverse diterpenes[1,5,6] and lignans along with phenylethanoid glycosides.[2]

I. ternifolius (D.Don) Kudô is one of the important traditional herbal plant in traditional Chinese medicine against

inflammation, icterohepatitis, enteritis, and diarrhoea[2] alongside hepatitis and hepatitis B infection.[5] Several unusual diterpenoids,[6–8] lignans, phenylethanoid glycosides,[2] triterpenes,[8] sterols,[9] spiroketones, and flavonoids[10] were isolated and identified through chemical characterization of various extracts from distinct *I. ternifolius* parts. Because of the plant's historic significance and documented chemical variety, several biological actions of plant extracts and/or metabolites involving anti-cancer activity have been reported[6–8,10,11] and the inhibition of DNA topoisomerase IB (TOP1) and tyrosyl-DNA phosphodiesterase 1 (TDP1).[8,9] Longikaurin A from *I. ternifolius* exerted anticancer activity against several cancer cell lines, specifically hepatocellular carcinoma cells.[10]

The present investigation described (i) ten new α-pyrone derivatives isolated and identified from the roots of *I. ternifolius* along with other known compounds, (ii) the absolute configuration of the isolated compounds by NMR, X-ray signal crystal, and electronic circular dichroism (ECD), and (iii) the growth inhibition of these compounds towards CCRF-CEM leukemia, MDA-MB-23 triple-negative breast cancer, and MCF7 breast cancer cell lines.

2. Results and discussion

2.1. Structure elucidation of isolated compounds

Ten new α-pyrones (**2–11**) along with further nine well-known compounds were isolated and identified from the dichloromethane–methanol (1 : 1) extract of the *I. ternifolius* roots *via*

aChemistry of Natural Compounds Department, National Research Centre, 33 El Bohouth St., Dokki, Giza, 12622, Egypt. E-mail: elshamynrc@yahoo.com

bChemistry of Medicinal Plants Department, National Research Centre, 33 El-Bohouth St., Dokki, Giza, 12622, Egypt. E-mail: mohegazy@uni-mainz.de

cFaculty of Pharmaceutical Sciences, Tokushima Bunri University, Yamashiro-cho, Tokushima, 770-8514, Japan. E-mail: umeyama@ph.bunri-u.ac.jp

dDepartment of Chemistry, Manipur Technical University, Takyelpat, Imphal, 795004, Manipur, India

eDepartment of Pharmaceutical Biology, Institute of Pharmaceutical and Biomedical Sciences, University of Mainz, Staudinger Weg 5, 55128, Mainz, Germany

† Electronic supplementary information (ESI) available. CCDC 2246696. For ESI and crystallographic data in CIF or other electronic format see DOI: https://doi.org/10.1039/d3ra03146b

different chromatographic and spectroscopic tools (Fig. 1). The known metabolites were characterized as (6R,5′R,6′S,1′R,2′R)-6-[5′,6′-diacetyloxy-1′-hydroxy-2′-methoxy-3E-heptenyl]-5,6-dihydro-2H-pyran-2-one (**1**),[12] synargentolide A (**12**),[13] hyptolide (**13**),[14,15] 6R-[5R,6S-diacetyloxy-1Z,3E-heptadienyl]-5,6-dihydro-2H-pyran-2-one (**14**),[16] oleanolic acid (**15**),[17] ursolic acid (**16**),[18,19] sodoponin (**18**),[20] rabdosianin B (**17**),[21,22] and acacetin (**19**).[23]

Compound **1** was identified using mass spectroscopy with low and high resolution, as well as NMR analysis. Comparing with the reported data,[12] the structure of **1** was confirmed as α-pyrone derivative, 6-[5′,6′-diacetyloxy-1′-hydroxy-2′-methoxy-3E-heptenyl]-5,6-dihydro-2H-pyran-2-one. The absolute configuration of **1** was constructed and confirmed by the X-ray single crystal diffraction of its bromobenzoate derivative (**S1**) (Fig. 2) and the positive ECD cotton effect at (Δε) 265.0 nm (+45.1). This detailed analysis allowed the unequivocal determination of **1** as (6R,5′R,6′S,1′R,2′R)-6-[5′,6′-diacetyloxy-1′-hydroxy-2′-methoxy-3E-heptenyl]-5,6-dihydro-

2H-pyran-2-one that was isolated previously from *Hyptis oblongifolia* leaves.[12]

The positive mode HRCIMS of **2** exhibited a molecular ion peak m/z at 315.1453 that revealed a molecular formula of $C_{15}H_{23}O_7$ (calc. 315.1444) and five unsaturation indexes. The presented ^{1}H NMR data in Table 1 revealed the existence of five aliphatic oxygenated methene protons at δ_H 4.44 dt (J = 6.1, 3.8 Hz), 3.57 dd (J = 2.2, 6.1 Hz), 3.72 dd (J = 4.0, 7.6 Hz), 4.05 t (J = 5.0 Hz), and 4.79 m, four olefinic methene protons at δ_H 5.88 dt (J = 1.6, 9.9 Hz), 6.97 dd (J = 5.7, 9.7 Hz), 5.66 dd (J = 7.7, 15.7 Hz), and 5.73 dd (J = 5.9, 15.8 Hz), one methylene at δ_H 2.45 m and one methyl protons at δ_H 1.11 d (J = 6.5 Hz). Also, two protons characteristic for two methyl groups were assigned in oxygenated systems, including methoxy and acetoxy groups, at respective δ_H 3.22 s and 1.93 s. Totally, 15 carbon resonances were characterized based on the ^{13}C NMR data (Table 2) and classified by the DEPT-135 and HSQC experiments. The careful assignments of these analyses yielded two quaternary carbons characteristic for two
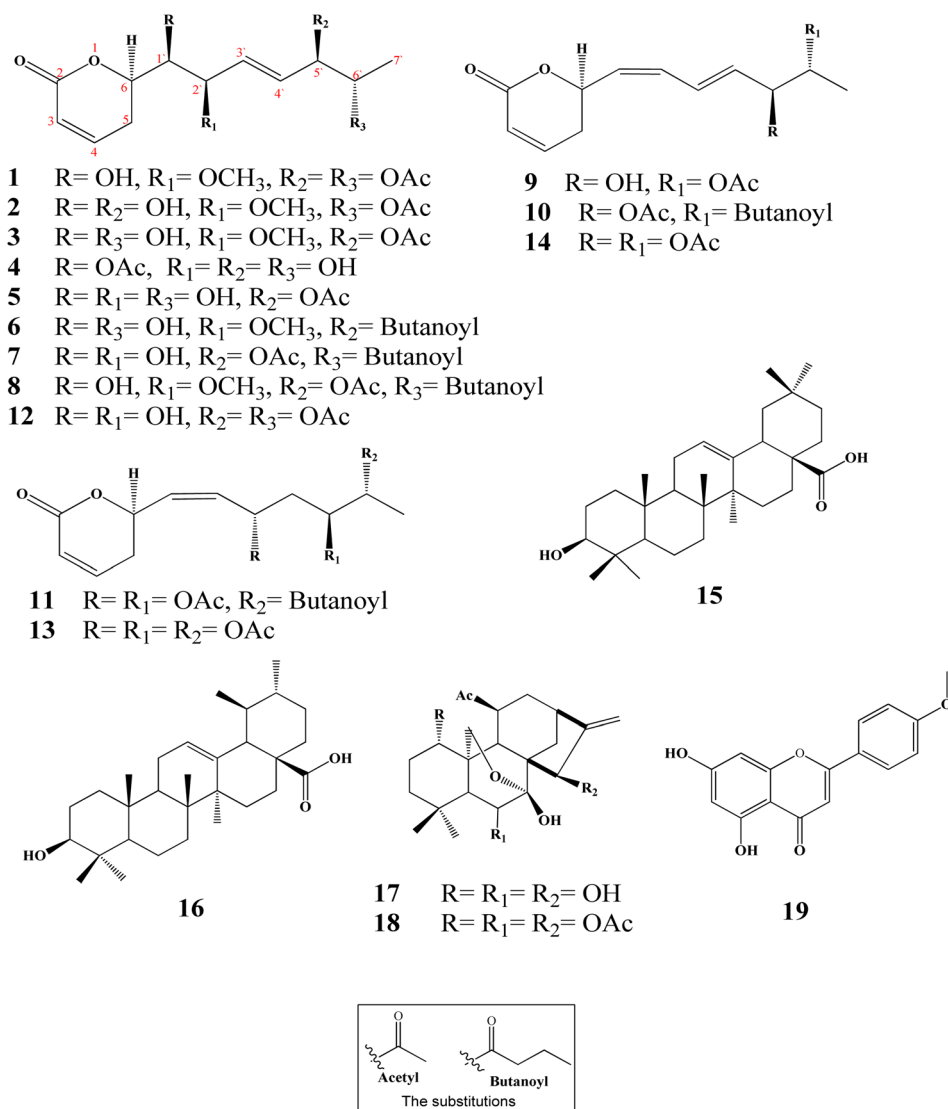

1 R= OH, R₁= OCH₃, R₂= R₃= OAc
2 R= R₂= OH, R₁= OCH₃, R₃= OAc
3 R= R₃= OH, R₁= OCH₃, R₂= OAc
4 R= OAc, R₁= R₂= R₃= OH
5 R= R₁= R₃= OH, R₂= OAc
6 R= R₃= OH, R₁= OCH₃, R₂= Butanoyl
7 R= R₁= OH, R₂= OAc, R₃= Butanoyl
8 R= OH, R₁= OCH₃, R₂= OAc, R₃= Butanoyl
12 R= R₁= OH, R₂= R₃= OAc

9 R= OH, R₁= OAc
10 R= OAc, R₁= Butanoyl
14 R= R₁= OAc

11 R= R₁= OAc, R₂= Butanoyl
13 R= R₁= R₂= OAc

15

16

17 R= R₁= R₂= OH
18 R= R₁= R₂= OAc

19

Acetyl **Butanoyl**
The substitutions

Fig. 1 Chemical structures of isolated metabolites from *I. ternifolius* roots.
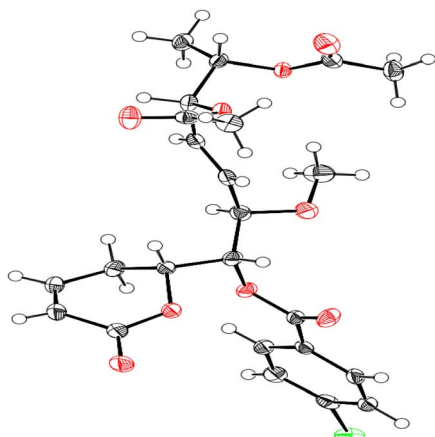
Fig. 2 X-ray single crystal diffraction of the bromobenzoate derivative of **1** (S1).

carbonyls at δ_C 164.9 (carbonyl of δ-lactone moiety) and δ_C 171.0 (acetoxyl carbonyl group), four olefinic methenes at δ_C (119.7, 129.1, 147.1, and 133.7), five oxygenated methenes at δ_C (73.0, 73.2, 74.3, 77.5, and 80.6), one aliphatic methylene at δ_C 24.7, one, and one methyl proton at δ_C 14.1, one methyl for acetoxy at δ_C

19.7, and one methyl of methoxy group at δ_C 55.6. All these data revealed that **2** has the same structure as **1** (ref. 12) except for the presence of only one acetoxyl substituent alongside two hydroxyl groups. The acetoxyl group was located in C-6′ depending upon the ^{1}H ^{1}H COSY correlations (Fig. 3) of the olefinic proton H-4′ at δ_H 5.73 dd ($J = 5.9$, 15.8 Hz) and the hydroxylated proton (H5′) at δ_H 4.05 t ($J = 5.0$ Hz), H-5′/H-6′ at δ_H 4.79 m, and H-6′ and methyl proton (H-7′) at δ_H 1.11 d ($J = 6.5$ Hz). The ^3J HMBC correlations (Fig. 3) between the H-4′/C-6′ (δ_C 73.0), H-6′/Ac-CO (δ_C 171.0), H-7′/ C-5′ (δ_C 73.2), H-5 (δ_H 2.45 m)/C-1′ (74.3), and H-3′(δ_H 5.66 dd ($J = 7.7$, 15.7 Hz))/C-1′ confirmed the localization of the acetoxyl group in C-6′ and the two hydroxyl groups in C-1′ and C-5′. Based upon these 1D and 2D NMR analyses, the structure of **2** was deduced as 6-[6′-acetyloxy-1′,5′-dihydroxy-2′-methoxy-3-heptenyl]-5,6-dihydro-2H-pyran-2-one. The *trans* (E) geometry of the C-3′/C-4′ olefinic system was confirmed by the discernible coupling constants of both sets of olefinic protons at 15.7 Hz.[12,13] Comparing with **1** and the literature,[12] the absolute orientation of **2** was affirmed *via* the coupling constants of the chiral carbons (Rahman and Gibbons, 2015 [16]) and the positive ECD cotton effect at ($\Delta\varepsilon$) 259.2 nm (+109.9). Thus, **2** was elucidated as (6R,5′R,6′S,1′R,2′R)-6-[6′-acetyloxy-1′,5′-dihydroxy-2′-methoxy-3E-heptenyl]-5,6-dihydro-2H-pyran-2-one (ternifolipyron A).

Table 1 ^{1}H NMR (500 Hz) spectral data of **2–8** [a]

No.	2	3	4	5	6	7	8
1	—	—	—	—	—	—	—
2	—	—	—	—	—	—	—
3	5.88 dt (1.6, 9.9)	5.87 dt (1.9, 9.8)	5.87 dt (1.9, 11.7)	5.88 dt (2.1, 9.9)	5.88 dt (1.7, 11.6)	5.87 ddd (1.2, 4.0, 8.6)	5.99 dt (2.0, 9.9)
4	6.97 dd (5.7, 9.7)	6.96 dt (4.4, 9.7)	6.98 dt (4.1, 13.9)	6.97 dd (3.2, 9.6)	6.96 dd (4.9, 9.7)	6.98 dddd (2.9, 5.6, 9.7)	7.09 dddd (4.2, 8.6, 10.0)
5	2.45 m	2.44 dddd (1.9, 4.2. 9.3)	2.47 m	2.47 m	2.44 m	2.46 m	2.57 m
6	4.44 dt (6.1, 3.8)	4.42 m	4.46 m	4.45 dd (5.5, 2.6)	4.43 m	4.44 t (2.6)	4.56 ddd (9.0, 9.0, 6.4)
1′	3.57 dd (2.2, 6.1)	3.58 dd (4.3, 13.3)	3.55 dd (3.7, 6.3)	3.57 dd (3.7, 6.4)	3.58 t (3.8)	3.55 dd (3.4, 6.4)	3.68 dd (3.8, 6.4)
2′	3.72 dd (4.0, 7.6)	3.72 dd (3.8, 7.6)	4.18 dd (3.8, 5.9)	4.18 d (3.8, 5.7)	3.71 dd (4.0, 7.9)	4.22 brt (4.2)	3.89 m
3′	5.66 dd (7.7, 15.7)	5.64 dd (7.5, 15.8)	5.80 dd (6.2, 15.7)	5.77 dd (6.1, 15.9)	5.64 dd (7.9, 15.8)	5.84 dddd (1.0, 5.9 15.8)	5.86 dd (7.4, 15.8)
4′	5.73 dd (5.9, 15.8)	5.72 dd (6.6, 15.8)	5.71 dd (6.3, 15.6)	5.73 dd (6.2, 13.3)	5.73 dd (6.8, 15.8)	5.69 dddd (1.3, 6.9, 15.8)	5.85 dd (6.0, 15.8)
5′	4.05 t (5.0)	5.06 dd (4.0, 6.5)	4.03 t (5.5)	5.08 dd (4.1, 6.5)	5.07 ddd (0.7, 4.2, 10.4)	5.30 dd (3.4, 7.0)	5.15 dddd (3.6, 6.6, 13.2)
6′	4.79 m	3.78 dd (4.0, 6.5)	4.78 m	3.76 dd (4.1, 6.4)	3.76 dd (4.5, 6.6)	4.99 dddd (3.4, 6.6, 13.2)	5.41 ddd (3.5, 5.0)
7′	1.11 d (6.5)	1.06 d (6.5)	1.08 d (6.5)	1.05 d (6.5)	1.06 d (6.5)	1.11 d (6.6)	1.25 d (6.6)
2′-OMe	3.22 s	3.19 s	—	—	3.21 s	—	3.33 br s

	6′-Ac		5′-Ac		1′-Ac		5′-Ac		6′-But		5′-Ac		5′-Ac	
CO	1.93 s	CO	1.99 s	CO	1.99 s	CO	1.98 s	CO	—	CO	—	CO	—
CH₃	—	CH₃	—	CH₃	—	CH₃	—	CH₂	2.26 t (7.4)	CH₃	1.95 s	CH₃	2.09 s
								CH₂	1.55 m	**6′-But**		**6′-But**	
								CH₃	0.86 t (7.4)	CO	—	CO	—
										CH₂	2.26 t	CH₂	2.31 t (7.3)
										CH₂	1.55 m	CH₂	1.65 m
										CH₃	0.86 t (7.4)	CH₃	0.97 t (7.4)

[a] All the compounds were measured in CD₃OD at 500 MHz; the coupling constants (J in Hz) are given in parentheses.
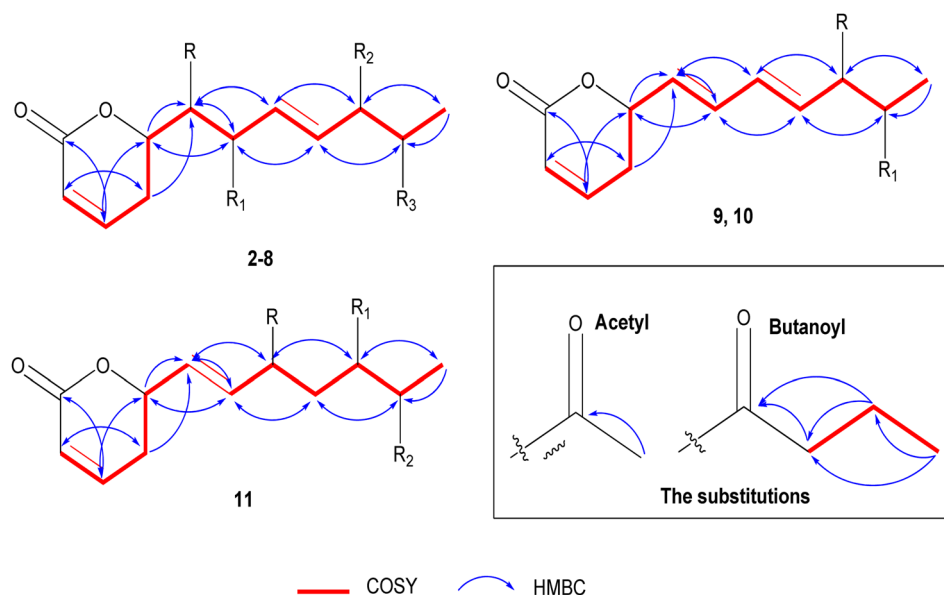
Table 2 ^{13}C NMR (125 Hz) spectral data of **2–8**

No.	2	3	4	5	6	7	8
1	—	—	—	—	—	—	—
2	164.9	164.9	165.0	165.0	164.9	165.0	164.8
3	119.7	119.7	119.7	119.7	119.7	119.8	119.8
4	147.1	147.1	147.2	147.2	147.1	147.2	147.1
5	24.7	24.6	24.9	24.9	24.6	25.1	24.9
6	77.5	77.5	77.6	77.6	77.5	77.5	77.4
1′	74.3	74.1	74.6	74.4	74.1	74.4	74.1
2′	80.6	80.7	70.4	70.4	80.7	70.1	80.4
3′	129.1	131.0	132.6	134.2	131.0	135.3	131.7
4′	133.7	129.8	130.3	126.5	130.1	125.1	128.5
5′	73.2	77.7	73.4	77.8	77.5	75.0	70.1
6′	73.0	68.1	73.1	68.3	68.2	70.4	74.7
7′	14.1	17.1	13.9	17.1	17.2	13.9	14.1
2′-OMe	55.6	55.6	—	—	55.6	—	55.8

	6′-Ac		5′-Ac		1′-Ac		5′-Ac		6′-But		5′-Ac		5′-Ac	
	CO	19.7	CO	19.6	CO	19.8	CO	19.7	CO	173.1	CO	170.4	CO	170.3
	CH$_3$	171.0	CH$_3$	170.7	CH$_3$	171.1	CH$_3$	170.8	CH$_2$	35.7	CH$_3$	19.5	CH$_3$	19.6
									CH$_2$	18.1	**6′-But**		**6′-But**	
									CH$_3$	12.5	CO	173.2	CO	173.1
											CH$_2$	35.7	CH$_2$	35.7
											CH$_2$	18.1	CH$_2$	18.1
											CH$_3$	12.5	CH$_3$	12.6

The positive mode HRCIMS of **3** showed a molecular ion peak m/z at 315.1453, indicating a molecular formula of $C_{15}H_{23}O_7$ (calc. 315.1444) with five unsaturation indexes. The assigned 1D NMR, including ^{1}H (Table 1) and ^{13}C NMR (Table 2) data, revealed that **3** had the same structure as **2**, with differences in the localization of the groups that were deduced *via* the variation of some protons and carbons. These variations were clearly observed in the downfield shift of H-5′/C-5′ by 1.01/4.5 ppm at δ_H 5.06 dd ($J = 4.0, 6.5$ Hz)/δ_C 77.7, the upfield shift of H-6′/C-5′ by 1.01/4.9 ppm at δ_H 3.78 dd ($J = 4.0, 6.5$ Hz)/δ_C 68.1 and C-7′ by 3.0 ppm at δ_C 17.1 indicating the presence of the acetoxyl group in C-6′ and the hydroxyl group in C-5′. These localizations were confirmed *via* ^{1}H ^{1}H COSY correlations (Fig. 3) of H-4′ (δ_H 5.72 dd ($J = 6.6, 15.8$ Hz))/H-5′ (δ_H 5.06 dd ($J =$

Fig. 3 Significant ^{1}H ^{1}H COSY and HMBC of **2–11**.

4.0, 6.5 Hz)), H-5′/H-6′ (δ_H 3.78 dd (J = 4.0, 6.5 Hz)), and H-6′/H-7′ (δ_H 1.06 d (J = 6.5 Hz)) along with the ^3J HMBC (Fig. 3) correlations of H-5′/Ac-CO (δ_C 170.7) and H-7′/C-5′ (δ_C 77.7). From above, **3** was constructed as 6-[5′-acetyloxy-1′,6′-dihydroxy-2′-methoxy-3-heptenyl]-5,6-dihydro-2H-pyran-2-one. As above compounds, the large coupling constants of the C-3′/C-4′ olefinic system sets at 15.8 Hz allowed its unequivocal geometry as *trans* (*E*).[12,13] The determination of the absolute configuration of **3** was carried out depending upon the comparing of the chiral carbons′ coupling constants with the literature[16] along with the positive ECD cotton effect at ($\Delta\varepsilon$) 261.8 nm (+83.4).[16] So, **3** was predicted as (6R,5′R,6′S,1′R,2′R)-6-[5′-acetyloxy-1′,6′-dihydroxy-2′-methoxy-3-heptenyl]-5,6-dihydro-2H-pyran-2-one (ternifolipyron B).

The HRCIMS of **4** in a positive mode exhibited a molecular ion peak m/z at 301.1265, confirming the molecular formula of $C_{14}H_{21}O_7$ (calc. 301.1209) and four unsaturation indexes. The overall data presented in 1D NMR (Tables 1 and 2) deduced that **4** was very close to the structure of **3** with some clear variations in the functional groups in the long chain. These significances were (i) the presence of three free hydroxy groups at C-2′, C5′, and C-6′ at δ_H/δ_C 4.18 dd (J = 3.8, 5.9 Hz)/70.4, 4.03 t (J = 5.5 Hz)/73.4 and 4.78 m/73.1, (ii) the absence of the methoxyl group that deduced *via* the downfield shift of H-2′ by 0.46 at δ_H 4.18 dd (J = 3.8, 5.9 Hz) and upfield of C-2′ by 9.8 ppm at δ_C 70.4, (iii) the upfield shift of the methyl proton, H-7′, by 3.1 ppm at δ_H 13.9, indicating that the only acetoxyl group was located in another carbon except C-6′. The localization of the acetoxyl group was affirmed in C-1′ *via* the ^1H ^1H COSY correlations of H-6 (δ_H 4.46 m)/H-1′ (δ_H 3.55 dd (J = 3.7, 6.3 Hz), H-1′/H-2′ (δ_H 4.18 dd (J = 3.8, 5.9 Hz) and H-2′/H-3′ (δ_H 5.80 dd (J = 6.2, 15.7 Hz) along with the ^3J HMBC correlations of H-1′/Ac-CO (δ_C 171.1), H-1′/C–H-5 (δ_C 24.9) and H-1′/C-3′ (δ_C 132.6) (Fig. 3). Hence, the structure of **4** was predicted as 6-[1′-acetyloxy-2′,5′,6′-trihydroxy-3-heptenyl]-5,6-dihydro-2H-pyran-2-one. As described for the above compounds, the H-3′/H-4′ olefinic system sets coupling constant at 15.7 Hz confirmed its *trans* (*E*) geometry.[13,16] Similar to above compounds, the absolute configuration of **4** was established based upon the positive ECD cotton effect at ($\Delta\varepsilon$) 258.0 nm (+46.2).[12] Thus, **4** was assigned as (6R,5′R,6′S,1′R,2′R)-6-[1′-acetyloxy-2′,5′,6′-trihydroxy-3-heptenyl]-5,6-dihydro-2H-pyran-2-one (ternifolipyron C).

Based upon the positive mode HRCIMS of **5**, which exhibited a molecular ion peak m/z at 301.1269, indicating a molecular formula of $C_{14}H_{21}O_7$ (calcd 301.1287) and four unsaturation indexes. By assignment of the ^1H (Table 1) and ^{13}C (Table 2) NMR data, **5** was affirmed to have the structure of **3** with only one exception, *i.e.*, the absence of the methoxylation in C-2′. This exception was assigned *via* the downfield shift of H-2′ by 0.46 ppm at δ_H 4.18 d (J = 3.8, 5.7 Hz), upfield shift of C-2′ by 9.7 ppm at δ_C 70.4, and the absence of the proton and carbon resonances of the methyl of methoxyl group. The ^1H ^1H COSY correlations (Fig. 3) of H-4′ (δ_H 5.72 dd (J = 6.6, 15.8 Hz))/H-5′ (δ_H 5.06 dd (J = 4.0, 6.5 Hz)), H-5′/H-6′ (δ_H 3.78 dd (J = 4.0, 6.5 Hz)), H-6′/H-7′ (δ_H 1.06 d (J = 6.5 Hz)) along with the ^3J HMBC (Fig. 3) correlations of H-5′/Ac-CO (δ_C 170.7) and H-7′/C-5′ (δ_C 77.7) confirmed the hydroxylation of C-1′, C-2′, and C-6′ along with

acetoxylation of C-5′. From these data, **5** was established as 6-[5′-acetyloxy-1′,2′,6′-trihydroxy-3-heptenyl]-5,6-dihydro-2H-pyran-2-one. As well, the *trans* (*E*) configuration of the C-3′/C-4′ olefinic system was constructed *via* the large coupling constants of both sets at 15.9 Hz.[12,13] The construction of the absolute stereochemistry of **5** was performed by the positive ECD cotton effect at ($\Delta\varepsilon$) 257.4 nm (+31.8).[12] So, **5** was predicted as (6R,5′R,6′S,1′R,2′R)-6-[5′-acetyloxy-1′,2′,6′-trihydroxy-3-heptenyl]-5,6-dihydro-2H-pyran-2-one (ternifolipyron D).

The positive mode HRCIMS molecular ion peak at m/z at 343.1755 of **6** revealed a molecular formula of $C_{17}H_{27}O_7$ (calc. 343.1757) alongside of five unsaturation indexes. The ^1H (Table 1) and ^{13}C (Table 2) NMR data of **6**, that exhibited seventeen carbon signals, affirmed that it was very close to **3** with only the exception of replacement of acetyl by butanoyl group in C-5′. The butanoyl group was determined *via* its characteristic ^1H/^{13}C signals at δ_H 2.26 t (J = 7.4 Hz)/δ_C 35.7, δ_H 1.55 m/δ_C 18.1, and δ_H 0.86 t (J = 7.4 Hz)/δ_C 12.5 in addition to its carbonyl at δ_C 173.1. The sequence of the butanoyl group was established by the ^1H ^1H COSY of the butanoyl protons, CH_3 (δ_H 0.86 t (J = 7.4 Hz)/CH_2 (δ_H 1.55 m), and CH_2 (δ_H 1.55 m)/CH_2 (δ_H 2.26 t (J = 7.4 Hz)), along with the ^3J HMBC (Fig. 3) correlations of CH_2 (δ_H 1.55 m)/CO (δ_C 173.1), and CH_3 (δ_H 0.86 (t (J = 7.4 Hz))/C_{H2} (δ_C 35.7). While the placement of butanoyl group in C-5′ was proven through ^3J HMBC (Fig. 3) correlation of H-5′ (δ_H 5.07 ddd (J = 0.7, 4.2, 10.4 Hz))/CO (δ_C 173.1). Based on these data, the structure of **6** was established as 6-[5′-butyroyl-1′,6′-dihydroxy-2′-methoxy-3-heptenyl]-5,6-dihydro-2H-pyran-2-one. The large coupling constants of the olefinic bond, C-3′/C-4′, at 15.8 Hz confirmed its *trans* (*E*) configuration.[12,13] Furthermore, the absolute configuration verification of **6** was achieved by the positive ECD cotton effect at ($\Delta\varepsilon$) 258.6 nm (+41.8).[13] So, **6** was predicted as (6R,5′R,6′S,1′R,2′R)-6-[5′-butyroyl-1′,6′-dihydroxy-2′-methoxy-3-heptenyl]-5,6-dihydro-2H-pyran-2-one (ternifolipyron E).

The molecular formula of **7** was predicted as $C_{17}H_{28}O_8$ (calc. 371.1706) from the HRCIMS molecular ion peak m/z at 371.1705, showing four unsaturation indexes. The structure of **7** was closely constructed as that of **5** *via* the ^1H (Table 1) and ^{13}C (Table 2) NMR data, except the presence of one acetoxyl and one butanoyl groups instead of one acetoxyl group in **5**. As described in **6**, the characterization of the butanoyl group was performed by the assigned ^1H/^{13}C signals as well as ^1H ^1H COSY and HMBC correlations (Fig. 3). The presence of the butanoyl group in C-6′ was confirmed *via* the downfield shift of H-6′/C-6′ by 1.23/2.1 ppm at δ_H 4.99 dddd (J = 3.4, 6.6, 13.2 Hz)/δ_C 70.4, along with the ^3J HMBC correlation (Fig. 3) of H-6′/CO (δ_C 173.2). Subsequently, the structure of **7** was assigned as 6-[5′-acetyloxy-6′-butyroyl-1′,2′-dihydroxy-3-heptenyl]-5,6-dihydro-2H-pyran-2-one. As described for all above compounds, the orientation of the olefinic system, C-3′/C-4′, was concluded as *trans* (*E*) from the large coupling constants at 15.8 Hz.[12,13] Also, the absolute stereochemistry of **7** was derived by means of ECD that exhibited a positive cotton effect at ($\Delta\varepsilon$) 259.2 nm (+94.7).[12] So, **7** was predicted as (6R,5′R,6′S,1′R,2′R)-6-[5′-acetyloxy-6′-butyroyl-1′,2′-dihydroxy-3-heptenyl]-5,6-dihydro-2H-pyran-2-one (ternifolipyron F).

The HRTOFESI-MS of **8** exhibited a molecular ion peak at *m/z* 407.1678, affirmed the molecular formula of $C_{19}H_{28}O_8Na$ (calc. 407.1682) and five unsaturation indexes. According to the [1]H (Table 1) and ^{13}C (Table 2) NMR data, the structure of **8** was closely identical to that of **1**, except for the existence of one acetoxyl and one butanoyl group instead of the two acetoxyl groups in **1**. As mentioned for the compounds above, the butanoyl group was validated by the assigned ^{1}H/^{13}C signals, ^{1}H ^{1}H COSY, and HMBC correlations (Fig. 3). Moreover, the buta-noyl group's location in C-6′ was confirmed by the [3]*J* HMBC correlation of H-6′ (δ_H 5.41 ddd (*J* = 3.5, 5.0 Hz))/CO (δ_C 173.1) (Fig. 3). After considering the aforementioned data, the struc-ture of **8** was determined to be 6-[5′-acetyloxy-6′-butyroyl-1′-hydroxy-2′-methoxy-3-heptenyl]-5,6-dihydro-2*H*-pyran-2-one. The C-3′/C-4′ olefinic system's orientation was determined to be *trans* (*E*) given a large coupling constant at 15.8 Hz as indicated in all of the compounds above.[12,13] The absolute stereochemistry of compound **8** was verified using the ECD, which showed a positive cotton effect at ($\Delta\varepsilon$) 257.8 nm (+104.8), in comparison to data from compound **1** and published data.[12] Thereby, the predicted structure of **8** was (6*R*,5′*R*,6′*S*,1′*R*,2′*R*)-6-[5′-acetyloxy-6′-butyroyl-1′-hydroxy-2′-methoxy-3-heptenyl]-5,6-dihydro-2*H*-pyran-2-one (ternifolipyron G).

Based on the molecular ion peak at *m/z* 267.1236 in the HRCIMS of **9**, the chemical formula was determined to be $C_{14}H_{19}O_5$ (calc. 267.1232), which revealed five unsaturation indices. Based upon the analysis of the ^{1}H and ^{13}C (Table 3) NMR data, which exhibited 14 carbon resonances, the structure of **9** was closely linked to that of **2**, with a few notable minor exceptions. These exceptions were summarized in (i) the pres-ence of two olefinic systems at δ_H 5.49 dd (*J* = 8.5, 11.0 Hz)/δ_C 127.1, δ_H 6.16 t (*J* = 11.0 Hz)/δ_C 131.9, δ_H 6.56 ddt (*J* = 1.0, 11.0, 15.2 Hz)/δ_C 125.9, and δ_H 5.76 dd (*J* = 6.5, 15.2 Hz)/δ_C 135.5, and (ii) the presence of the only two functional groups in the hep-tanyl chain, including one hydroxyl at δ_H 4.10 ddd (*J* = 1.0, 4.4, 6.5 Hz)/δ_C 73.3 and one acetoxyl at δ_H 4.78 m/δ_C 73.0. In addi-tion to the C-3′/C-4′ olefinic system in all above compounds, the other olefinic system was located in C-1′/C-2′ based upon the ^{1}H ^{1}H COSY correlations (Fig. 3) of H-6 (δ_H 5.40 m)/H-1′ (δ_H 5.49 dd (8.5, 11.0)), H-1′/H-2′ (δ_H 6.16 t (*J* = 11.0 Hz)), H-2′/H-3′ (δ_H 6.56 ddt (*J* = 1.0, 11.0, 15.2 Hz)), H-3′, H-4′ (δ_H 5.76 dd (*J* = 6.5, 15.2 Hz)). The site of C-1′/C-2′ olefinic system was assured by [3]*J* HMBC correlations (Fig. 3) of the H-5 (δ_H 2.38 m)/C-1′ (δ_C 127.1), H-6/C-2′ (δ_C 131.9), H-1′/C-3′ (δ_C 125.9), and H-2′/C-4′ (δ_C 135.5). Also, the presence of the hydroxyl and acetoxyl groups in C-5′ and C-6′, respectively, was confirmed by the same described ^{1}H ^{1}H COSY and HMBC correlations in compound **2**. After taking all aforementioned information into account, the structure of **9** was determined to be 6-[6′-acetyloxy-5′-hydroxy-1,3-hepta-dienyl]-5,6-dihydro-2*H*-pyran-2-one. According to what was

Table 3 ^{1}H and ^{13}C NMR spectral data of **9–11** [a]

No.	9 δ_H	9 δ_C	10 δ_H	10 δ_C	11 δ_H	11 δ_C
1	—	—	—	—	—	—
2	—	165.2	—	165.0	—	164.6
3	5.92 dd (1.6, 10.0)	120.1	5.92 dd (1.7, 9.8)	120.1	5.92 dddd (1.0, 2.6, 7.2, 9.8)	120.1
4	6.96 m	146.6	6.95 m	146.5	6.97 m	146.3
5	2.38 m	29.4	2.37 m	29.3	2.33 m, 2.43 m	29.4
6	5.40 m	74.2	5.39 m	74.1	5.32 m	74.4
1′	5.49 dd (8.5, 11.0)	127.1	5.55 t (8.7, 10.9)	128.5	5.64 t (7.9, 10.6)	129.9
2′	6.16 t (11.0)	131.9	6.16 t (11.1)	131.2	5.49 dd (1.1, 10.6)	130.9
3′	6.56 ddt (1.0, 11.0, 15.2)	125.9	6.59 ddt (1.0, 11.3, 15.2)	128.6	5.45 dd (3.6, 9.5)	65.9
4′	5.76 dd (6.5, 15.2)	135.5	5.73 dd (7.3, 15.2)	130.1	1.73 m, 1.89 m	35.0
5′	4.10 ddd (1.0, 4.4, 6.5)	73.3	5.33 dddd (1.0, 3.6, 3.8, 7.3)	75.0	5.00 m	70.6
6′	4.78 m	73.0	5.00 m	70.3	4.89 dd (4.9, 6.5)	70.6
7′	1.08 d (6.5)	13.9	1.09 d (6.6)	14.0	1.08 d (6.5)	15.0

6′-Ac			**5′-Ac**		**4′-Ac**	
CO	—	171.0	CO — 170.3		CO — 170.6	
CH_3	1.96 s	19.7	CH_3 1.93 s 19.5		CH_3 1.90 s 19.4	
			6′-But		**5′-Ac**	
			CO — 173.2		CO — 170.8	
			CH_2 2.18 t (7.4) 35.7		CH_3 1.94 s 19.5	
			CH_2 1.53 m 18.1		**6′-But**	
			CH_3 0.85 t (7.5) 12.5		CO — 173.0	
					CH_2 2.20 t (7.3) 35.7	
					CH_2 1.54 m 18.1	
					CH_3 0.85 t (7.4) 12.5	

[a] All the compounds were measured in CD₃OD at 500 MHz; the coupling constants (*J* in Hz) are given in parentheses.

previously stated, the significant coupling constant at 15.7 Hz validated the geometry of the C-3′/C-4′ olefinic system as *trans* (*E*).[12,13] In contrast, the C-1′/C-2′ olefinic system's geometry was predicted to be *cis* (*Z*) according to the modest coupling constant at 11.0 Hz in both sites.[13,14,24] The absolute configuration of **9** was ascertained by the ECD study, which showed a positive cotton effect at ($\Delta\varepsilon$) 264.0 nm (+35.3) by comparison with compound **1**, other compounds, and the literature.[12] With the aforementioned information, **9** was ultimately determined as (6*R*,5′*R*,6′*S*)-6-[6′-acetyloxy-5′-hydroxy-1*Z*,3*E*-heptadienyl]-5,6-dihydro-2*H*-pyran-2-one (ternifolipyron H).

Compound **10**'s TOFESIMS results showed a molecular ion peak at *m/z* 359.1465 that revealed the molecular formula to be $C_{18}H_{24}O_6Na$ (calc. 359.1471) and six unsaturation indices. The study of the ^{1}H and ^{13}C (Table 3) NMR data, which showed 18 carbon resonances, revealed that compound **10**'s structure was largely similar to compound **9**'s, with a few significant minor deviations. These changes could be clearly seen when there was only one butanoyl group and one acetoxyl group present. The [3]*J* HMBC correlation (Fig. 3) of H-5′ (δ_H 5.33 dddd (*J* = 1.0, 3.6, 3.8, 7.3 Hz))/Ac-CO (δ_C 170.3) corroborated the placement of the acetoxyl group in C-5′. The butanoyl group was created, as mentioned for the aforementioned compounds by the ^{1}H ^{1}H COSY and HMBC correlations (Fig. 3) of its protons and carbons. The [3]*J* HMBC correlations (Fig. 3) of the H-6′ (δ_H 5.00 m)/But-CO (δ_C 173.2) showed that the butanoyl group existed in C-6′. The olefinic systems, C-1′/C-2′ and C-3′/C-4′, in **10** were confirmed by the same in **9**. Based on the data discussed above, **10** was chemically created as 6-[5′-acetyloxy-6′-butyroyl-1,3-heptadienyl]-5,6-dihydro-2*H*-pyran-2-one. The *cis* (*Z*) and *trans* (*E*) geometries of the olefinic systems were confirmed by the coupling constants of C-1′/C-2′ and C-3′/C-4′, respectively, at 10.9 and 15.2 Hz.[12–14,24] In a similar way, the absolute configuration of **10** was established using the ECD experimental data, which revealed a positive cotton effect at ($\Delta\varepsilon$) 264.0 nm (+76.9).[14] Based on the information above, **10** was eventually (6*R*,5′*R*,6′*S*)-6-[5′-acetyloxy-6′-butyroyl-1*Z*,3*E*-heptadienyl]-5,6-dihydro-2*H*-pyran-2-one (ternifolipyron I).

From the HRCIMS molecular ion peak at *m/z* 397.1871, compound **11**'s molecular formula was inferred to be $C_{20}H_{29}O_8$ (calc. 397.1862) coupled with six unsaturation indices. The **11**'s ^{1}H and ^{13}C (Table 3) NMR data, which displayed 20 carbon signals, demonstrated that it was largely similar to **10**, with prominent variations. These two variations were located in the heptanyl chain as follows: (i) presence of only one olefinic system, and (ii) the existence of a new acetoxylated carbon at δ_H 5.45 dd (*J* = 3.6, 9.5 Hz)/δ_C 65.9 along with one methylene carbon at δ_H 1.73 m, 1.89 m/δ_C 35.0. The olefinic system was demonstrated to be C-1′/C-2′ by the ^{1}H ^{1}H COSY correlations (Fig. 3) of the H-6 (δ_H 5.32 m)/H-1′ (δ_H 5.64 t (*J* = 7.9, 10.6 Hz)), H-1′/H-2′ (δ_H 5.49 dd (*J* = 1.1, 10.6 Hz)) along with the [3]*J* HMBC correlation (Fig. 3) of H-1′/C-5 (δ_C 29.4). Furthermore, the new acetoxylated carbon and methylene carbon were localized in C-3′ and C-4′, respectively, depending on the ^{1}H ^{1}H COSY correlations (Fig. 3) of the H-2′/H-3′ (δ_H 5.45 dd (*J* = 3.6, 9.5 Hz)), H-3′/H-4′ (δ_H 1.73 m, 1.89 m), and H-4′/H-5′ (δ_H 5.00 m) as well as the [3]*J* HMBC correlation (Fig. 3) of H-1′/C-3 (δ_C 65.9), H-4′/C-2′ (δ_C 130.9), and H-3′/Ac-CO (δ_C 170.6). The other sections of this compound, including 5′-acetoxyl and 6′-butyroyl, were determined as described for **10**. Thus, **11** was established as 6-[6′-butyroyl-3′,5′-diacetyloxy-1-heptadienyl]-5,6-dihydro-2*H*-pyran-2-one. The C-1′/C-2′ olefinic system's *cis* (*Z*) geometry was decided by the system's modest coupling constant at 10.6 Hz.[13,14,24] Also, **11**′ absolute configuration was defined depending upon the positive cotton effect at ($\Delta\varepsilon$) 257.8 nm (+91.2) in the ECD experimental data.[14] Therefore, **11** was determined as (6*R*,3′*R*,5′*R*,6′*S*)-6-[6′-butyroyl-3′,5′-diacetyloxy-1*Z*-heptenyl]-5,6-dihydro-2*H*-pyran-2-one (ternifolipyron J).

2.2. Cytotoxic activity of isolates

All isolated compounds were initially screened against CCRF-CEM leukemia cell lines at one fixed concentration (30 μM) (Fig. 4). The compounds **7**, **10**, **12**, and **15–17** were the most effective metabolites with this fixed concentration (30 μM). As a next step, dose–response curves were performed with concentrations in a range from 0.001 to 100 μg mL^{-1} for three cancer cell lines (CCRF-CEM, MDA-MB-23, MCF7). Ursolic acid (**16**) exhibited the strongest cytotoxic activity against three cancer cell lines as follows: the IC$_{50}$ for the three cell lines were 8.37 μM, 18.04 μM, and 18.93 μM, respectively (Fig. 5).
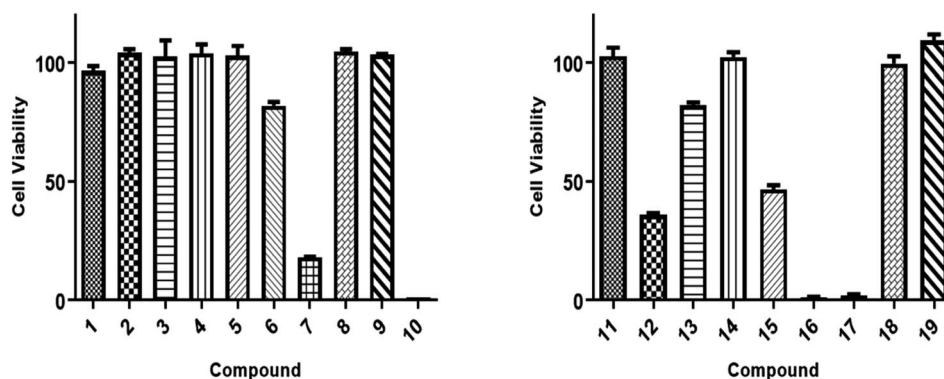

Fig. 4 Cytotoxic activity screening results of isolates (**1–19**) against CCRF-CEM cancer cells at 30 μg mL^{-1} as a fixed concentration. Three different experiments' average and error bars are displayed in bars. The paired Student's *t*-test was used for statistical analysis.
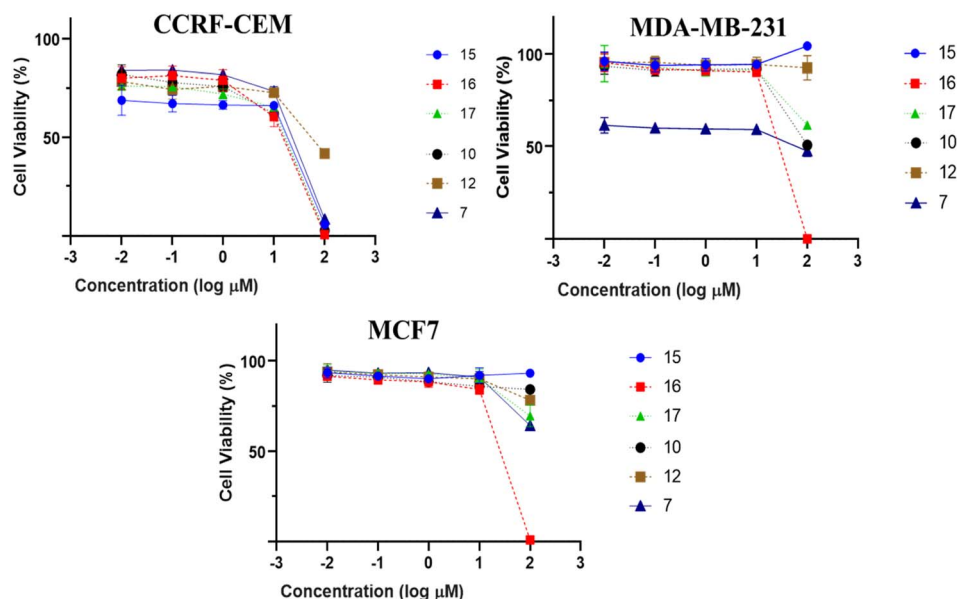
Fig. 5 Dose response curves of isolates (**1–19**) against CCRF-CEM leukemia, MDA-MB-231 triple-negative breast cancer and MCF7 a breast cancer cells by resazurin assessment. Mean values and standard deviations of each three independent experiments with each six parallel measurements are shown.

3. Experimental

3.1. General experimental procedures

Silica gel 60 (230–400 and 100–200 mesh), pre-coated Kieselgel-60 F-254-TLC plates silica gel (Merck, Darmstadt, Germany), and Sephadex LH-20 (Pharmacia Co. Ltd) were used as packing materials for column chromatography. Isolera-one flash chromatography (Biotage; Suite C Charlotte, NC; USA) was used for flash chromatographic analysis as well as the isolation and purification processes. The compounds were purified using HPLC with a Jasco-pump (PU-980) equipped with a Jasco UV-970 intelligent detector (UV/VIS) at 210 nm. A HPLC semi-preparative Supelco C18-RP-column (250 × 10 mm, 5 μm) was also used. The optical rotation of the isolated compounds was measured by a JASCO (P-2300) polarimeter (Tokyo, Japan). A Bruker 500 Hz (MA, USA) spectrometer was used for recording the 1D NMR, including ^{1}H, ^{13}C, and DEPT-135, and the 2D NMR, including HSQC, HMBC, ^{1}H ^{1}H COSY, and NOESY. All NMR analyses were measured in deuterated methanol (CD$_3$OD) at room temperature. The chemical shifts and coupling constants were given in delta (δ, ppm) and Hertz (Hz), respectively. CD$_3$OD was referenced at δ_H 4.77 and δ_H 3.31 ppm in ^{1}H NMR, and at δ_C 49.14 in ^{13}C NMR. The experimentally measured electronic circular dichroism (ECD) of the compounds were measured in CH$_3$OH by a JASCO-810 spectrometer. The mass spectral data including, LR and HR-MS, were derived by a JEOL (JMS-700) instrument (Tokyo, Japan).

3.2. Plant material

The roots of *I. ternifolius* were collected in West Imphal, Manipur, India, 24.6637° N, 93.9063° E, during March/April 2020. The identification and authen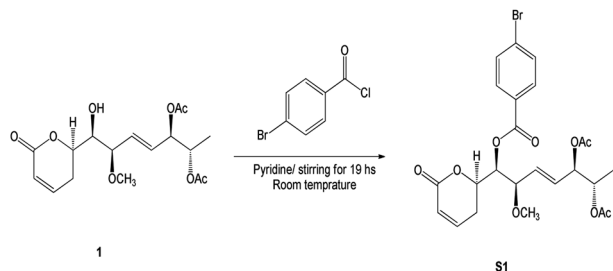tication of the collected plant were kindly performed by Dr Biseshwori Thongam, Taxonomist, Bioresource and Sustainable Development Institute, IBSD Imphal, Manipur, India. A plant voucher (No.: IBSD/Z-ITF-1578) was stored at the Plant Bioresource Division Herbarium, IBSD Imphal, India.

3.3. Extraction process

I. ternifolius roots were carefully cleaned, left for one week in a dry and shady place at room temperature until complete dryness, and then crushed using a clean plant grindery into fine powder. The extraction of the powdered roots (1.3 kg) occurred by maceration in dichloromethane-methanol (CH$_2$Cl$_2$–MeOH, 6 L) at room temperature for successive 72 h and filtered. The filtrate was extracted with the same steps two more times. The total extract (84.5 g) was obtained as black gum by complete drying of the overall amount of liquid extract under vacuum at 45–50 °C.

3.4. Metabolite isolation and purification

The extract was subjected to rapid fractionation over silica gel (230–400 mesh) column chromatography (CC) starting with *n*-hexane/CH$_2$Cl$_2$ (1/0, 4/1, 3/2, 2/3, 1/4, 0/1) followed by CH$_2$CL$_2$/MeOH (4/1, 3/2, 2/3, 0/1) as elution systems afforded 46 fractions. These fractions were collected to 8 main fractions (designated YGS-1 to YGS-8) after examination with thin layer chromatography (TLC) with different solvent systems. Fraction YGS-4 (1.4 g) was fractionated over Isolera-one flash CC using a step gradient of CHCl$_3$/MeOH that yielded compound **1** (178.7 mg) along with three sub-fractions (YGS-4A, YGS-4B, and YGS-4C). The further fractionation of YGS-4A (152.1 mg) with a mixture of CHCl$_3$/MeOH (1 : 1) as an elution system over Sephadex LH-20 CC yielded **2** (7.9 mg), **3** (8.5 mg), **4** (10.2 mg),

Scheme 1 Synthetic of (6R,5′R,6′S,1′R,2′R)-6-[5′,6′-diacetyloxy-1′-((4-bromobenzoyl)oxy)-2′-methoxy-3E-heptenyl]-5,6-dihydro-2H-pyran-2-one (S1).

and **18** (17.6 mg). Fraction YGS-4B (131.2 mg) was carefully filtered, and then the clearly soluble portion was subjected to C18-RP-HPLC with an eluting system of MeOH–H₂O (3 : 2) to yield **5** (13.4 mg), **6** (11.6 mg), and **7** (9.8 mg). With the same sequence, **9** (7.7 mg), **12** (56.8 mg), and **19** (143.2 mg) were purified from the fraction YGS-4C (94.3 mg). The filtrated methanol-soluble portion of fraction YGS-2 (1.0 g) was subjected to C18-RP-HPLC using MeOH/H₂O (4 : 1) as eluting system and yielded **8** (14.3 mg), **15** (46.1 mg), and **16** (53.5 mg). The further fractionation of fraction YGS-3 (1.3 g) over silica gel CC using CHCl₃/MeOH (1/0, 9/1, 4/1, 7/3, 3/2, 1/1, 2/3, and 0/1) yielded **17** (161.4 mg), **14** (128.2 mg), and sub-fraction YGS-3A. The eluting of the sub-fraction YGS-3A (68.7 mg) by MeOH–H₂O (3 : 2) as the mobile phase using the C18-RP-HPLC led to the purification of **10** (12.4 mg), **11** (16.1 mg), and **13** (33.7 mg).

3.5. Preparation of bromobenzoyl derivative of 1

The *p*-bromobenzoyl chloride (13.3 mg, 0.06 mmol) was added to a solution of compound **1** (1.5 mg, 4.3 μmol) in dried pyridine (0.1 mL). After stirring for 19 h, at room temperature, the resulting solution was diluted with ethyl acetate and washed with aqueous KHSO₄ (1 M) and aqueous saturated NaHCO₃ (Scheme 1). The resulting organic layer was dried over anhydrous Na₂SO₄, filtrated, and concentrated under vacuum. The crude residue was purified by silica gel chromatography to give benzoate **S1** (2.3 mg, 4.3 μmol) in quantitative yield as a colourless oil.

3.6. X-ray single crystallographic procedure of S1

Single crystals of bromobenzoate derivative of **1** (S1) were obtained by slow evaporation of a hexane and ethyl acetate solution, selected and fitted onto a glass fiber, and measured at −173 °C with a Bruker Apex II ultra diffractometer using MoKα radiation. Data correction and reduction were performed with the crystallographic package Apex II. The structure was solved and refined using the Bruker SHELXTL software package. All non-hydrogen atoms were refined anisotropically, and hydrogen atoms were positioned geometrically. The final anisotropic full-matrix least-squares refinement on F^2 with 311 variables converged at $R_1 = 2.51\%$, for the observed data and $wR_2 = 5.92\%$ for all data. The ORTEP plot was obtained by the program PLATON (A. L. Spek, 2009). Crystallographic data

(excluding structure factors) for the structures of **S1** have been deposited with the Cambridge Crystallographic Data Centre as supplementary publication numbers CCDC 2246696.†

3.7. Spectroscopic data of isolates (1–11)

(6R,5′R,6′S,1′R,2′R)-6-[5′,6′-Diacetyloxy-1′-hydroxy-2′-methoxy-3E-heptenyl]-5,6-dihydro-2H-pyran-2-one (1). Pale yellow oil; ([α]₂₅D +16.1; *c* 0.1, MeOH); ECD (MeOH; *c* mg mL⁻¹) (Δε) + 45.1 (265.0 nm); the spectroscopic spectra including LREIMS & TOFESIMS, ¹H (500 Hz), ¹³C NMR (125 Hz; CD₃OD) (Fig. S1–S4†), and ECD (Fig. S94†) were inserted in the ESI data file.†

(6R,5′R,6′S,1′R,2′R)-6-[5′,6′-Diacetyloxy-1′-((4-bromobenzoyl)oxy)-2′-methoxy-3E-heptenyl]-5,6-dihydro-2H-pyran-2-one (S1). Colorless oil, ¹H (300 Hz): ¹H NMR (300 MHz in CDCl₃) δ_H 7.91 (m, 2H), 7.61 (m, 2H), 6.88 (ddd, *J* = 9.7, 5.3, 2.9 Hz, 1H), 6.06 (br d, *J* = 9.7 Hz, 1H), 5.78 (dd, *J* = 15.6, 7.1 Hz, 1H), 5.61 (dd, *J* = 15.6, 6.8 Hz, 1H), 5.38 (dd, *J* = 8.2, 2.6 Hz, 1H), 5.23 (dd, *J* = 7.1, 3.5 Hz, 1H), 4.99 (qd, *J* = 6.5, 3.5 Hz, 1H), 4.90 (ddd, *J* = 10.3, 8.2, 5.3 Hz, 1H), 4.25 (dd, *J* = 6.8, 2.6 Hz, 1H), 3.37 (s, 3H), 2.47–2.40 (m, 2H), 2.01 (s, 3H), 1.87 (s, 3H), 1.07 (d, *J* = 6.5 Hz, 3H). Crystal data: C₂₄H₂₇BrO₉, MW = 539.36, monoclinic, space group P2₁, Z = 2, *a* = 13.5903 (13) Å, *b* = 6.6575 (6) Å, *c* = 13.8833 (13) Å, *β* = 100.1930 (10)°, *V* = 1236.3 (2) Å³, Flack parameter = 0.020 (4), GOF = 0.937. The spectroscopic spectra including ¹H NMR (300 Hz, Fig. S5†) was inserted in the ESI data file.†

Ternifolipyron A (2). Golden yellow oil; ([α]₂₅D +29.2; *c* 0.1, MeOH); ECD (MeOH; *c* mg mL⁻¹) (Δε) + 109.9 (259.2 nm); ¹H NMR (500 Hz; CD₃OD) and ¹³C NMR (125 Hz; CD₃OD): presented in Tables 1 and 2, CIMS, *m/z* (rel. int.): 315 [M + 1]⁺ (22%), 297 (37%), 255 (21%), 233 (54%), 205 (42%), 181 (44%), 163 (34%), 127 (63%); 111 (83%); 99 (43%); 95 (100%); 43 (26%); 41 (59%); HRCIMS *m/z* 315.1453 (C₁₅H₂₃O₇, calcd 315.1444). Unsaturation indexes: 5. The spectral data involving the LR & HRCIMS, 1D, 2D NMR (Fig. S6–S14†) and ECD (Fig. S94†) were inserted in the ESI data file.†

Ternifolipyron B (3). Pale yellow gummy oil; ([α]₂₅D +22.7; *c* 0.1, MeOH); ECD (MeOH; *c* mg mL⁻¹) (Δε) + 83.4 (261.8 nm); ¹H NMR (500 Hz; CD₃OD) and ¹³C NMR (125 Hz; CD₃OD): presented in Tables 1 and 2, CIMS, *m/z* (rel. int.): 315 [M + 1]⁺ (7%), 297 (22%), 255 (20%), 238 (21%), 223 (46%), 205 (26%), 181 (84%), 163 (41%), 155 (46%), 127 (64%); 111 (65%); 99 (43%); 95 (100%); 69 (26%); 45 (22%); 41 (43%); HRCIMS *m/z* 315.1453 (C₁₅H₂₃O₇, calcd 315.1444). Unsaturation indexes: 5. The spectral data involving the LR & HRCIMS, 1D, 2D NMR (Fig. S15–S23†) and ECD (Fig. S94†) were inserted in the ESI data file.†

Ternifolipyron C (4). Dark yellow gum; ([α]₂₅D +22.7; *c* 0.1, MeOH); ECD (MeOH; *c* mg mL⁻¹) (Δε) + 46.2 (258.0 nm); ¹H NMR (500 Hz; CD₃OD) and ¹³C NMR (125 Hz; CD₃OD): presented in Tables 1 and 2, CIMS, *m/z* (rel. int.): 301 [M + 1]⁺ (4%), 283 (31%), 223 (55%), 205 (47%), 181 (64%), 163 (44%), 141 (36%), 128 (68%), 113 (47%); 97 (92%); 95 (100%); 86 (46%); 81 (38%); 69 (48%); 43 (45%); 41 (48%); HRCIMS *m/z* 301.1265 (C₁₄H₂₁O₇, calcd 301.1209). Unsaturation indexes: 4. The spectral data involving the LR & HRCIMS, 1D, 2D NMR (Fig. S24–S32†) and ECD (Fig. S94†) were inserted in the ESI data file.†

Ternifolipyron D (5). Dark yellow oil; ($[\alpha]_{25}^{D}$ +29.4; c 0.1, MeOH); ECD (MeOH; c mg mL^{-1}) ($\Delta\varepsilon$) + 31.8 (257.4 nm); ^{1}H NMR (500 Hz; CD$_3$OD) and ^{13}C NMR (125 Hz; CD$_3$OD): presented in Tables 1 and 2, CIMS, m/z (rel. int.): 301 [M + 1]$^+$ (17%), 283 (56%), 223 (100%), 205 (45%), 198 (58%), 181 (67%), 127 (100%), 111 (71%), 97 (90%); 95 (97%); 86 (54%); 81 (51%); 69 (45%); 43 (53%); 41 (98%); HRCIMS m/z 301.1269 (C$_{14}$H$_{21}$O$_7$, calcd 301.1287). Unsaturation indexes: 4. The spectral data involving the LR & HRCIMS, 1D, 2D NMR (Fig. S33–S41†) and ECD (Fig. S94†) were inserted in the ESI data file.†

Ternifolipyron E (6). Pale brown gum; ($[\alpha]_{25}^{D}$ +20.0; c 0.1, MeOH); ECD (MeOH; c mg mL^{-1}) ($\Delta\varepsilon$) + 41.8 (258.6 nm); ^{1}H NMR (500 Hz; CD$_3$OD) and ^{13}C NMR (125 Hz; CD$_3$OD): presented in Tables 1 and 2, CIMS, m/z (rel. int.): 343 [M + 1]$^+$ (18%), 325 (45%), 297 (27%), 255 (42%), 223 (62%), 183 (63%), 181 (100%), 169 (68%), 163 (49%), 127 (89%), 111 (85%), 99 (41%); 95 (86%); 81 (30%); 71 (64%); 43 (57%); 41 (28%); HRCIMS m/z 343.1755 (C$_{17}$H$_{27}$O$_7$, calcd 343.1757). Unsaturation indexes: 5. The spectral data involving the LR & HRCIMS, 1D, 2D NMR (Fig. S42–S50†) and ECD (Fig. S94†) were inserted in the ESI data file.†

Ternifolipyron F (7). Pale brown gum; ($[\alpha]_{25}^{D}$ +20.5; c 0.1, MeOH); ECD (MeOH; c mg mL^{-1}) ($\Delta\varepsilon$) + 94.7 (259.2 nm); ^{1}H NMR (500 Hz; CD$_3$OD) and ^{13}C NMR (125 Hz; CD$_3$OD): presented in Tables 1 and 2, CIMS, m/z (rel. int.): 371 [M + 1]$^+$ (6%), 353 (17%), 311 (100%), 223 (51%), 205 (38%), 183 (43%), 155 (45%), 141 (38%), 128 (64%), 113 (46%), 97 (65%), 95 (100%); 81 (41%); 71 (95%); 43 (39%); 41 (67%); HRCIMS m/z 371.1705 (C$_{17}$H$_{28}$O$_8$, calcd 371.1706). Unsaturation indexes: 3. The spectral data involving the LR & HRCIMS, ECD, 1D, 2D NMR (Fig. S51–S59†) and ECD (Fig. S94†) were inserted in the ESI data file.†

Ternifolipyron G (8). Yellow gum; ($[\alpha]_{25}^{D}$ +22.7; c 0.1, MeOH); ECD (Me OH; c mg mL^{-1}) ($\Delta\varepsilon$) + 104.8 (257.8 nm); ^{1}H NMR (500 Hz; CD$_3$OD) and ^{13}C NMR (125 Hz; CD$_3$OD): presented in Tables 1 and 2, HRTOFESIMS m/z 407.1678 (C$_{19}$H$_{28}$O$_8$Na, calcd 407.1682). Unsaturation indexes: 5. The spectral data involving the TOFESIMS, ECD, 1D, 2D NMR (Fig. S60–S67†) and ECD (Fig. S94†) were inserted in the ESI data file.†

Ternifolipyron H (9). Dark yellow oil; ($[\alpha]_{25}^{D}$ +20.5; c 0.1, MeOH); ECD (MeOH; c mg mL^{-1}) ($\Delta\varepsilon$) + 35.3 (264.0 nm); ^{1}H NMR (500 Hz; CD$_3$OD) and ^{13}C NMR (125 Hz; CD$_3$OD): presented in Table 3, CIMS, m/z (rel. int.): 267 [M]$^+$ (5%), 249 (65%), 189 (100%), 180 (47%), 171 (36%), 162 (74%), 147 (42%), 133 (58%), 121 (20%), 105 (24%), 95 (25%), 81 (34%); 43 (66%); 41 (62%); HRCIMS m/z 267.1236 (C$_{14}$H$_{19}$O$_5$, calcd 267.1232). Unsaturation indexes: 5. The spectral data involving the LR & HRCIMS, 1D, 2D NMR (Fig. S68–S76†) and ECD (Fig. S94†) were inserted in the ESI data file.†

Ternifolipyron I (10). Dark yellow oil; ($[\alpha]_{25}^{D}$ +24.3; c 0.1, MeOH); ECD (MeOH; c mg mL^{-1}) ($\Delta\varepsilon$) + 76.9 (264.0 nm); ^{1}H NMR (500 Hz; CD$_3$OD) and ^{13}C NMR (125 Hz; CD$_3$OD): presented in Table 3, HRTOFESIMS m/z 359.1465 (C$_{18}$H$_{24}$O$_6$Na, calcd 359.1471). Unsaturation indexes: 5. The spectral data involving the TOFESIMS, 1D, 2D NMR (Fig. S77–S84†) and ECD (Fig. S94†) were inserted in the ESI data file.†

Ternifolipyron J (11). Golden yellow oil; ($[\alpha]_{25}^{D}$ +32.1; c 0.1, MeOH); ECD (MeOH; c mg mL^{-1}) ($\Delta\varepsilon$) + 91.1 (257.8 nm); ^{1}H NMR (500 Hz; CD$_3$OD) and ^{13}C NMR (125 Hz; CD$_3$OD): presented in Table 3, CIMS, m/z (rel. int.): 397 [M + 1]$^+$ (10%), 337 (100%), 329 (24%), 277 (64%), 249 (19%), 239 (43%), 207 (57%), 189 (66%), 179 (18%), 171 (22%), 162 (24%), 151 (22%), 71 (26%), 45 (23%), 43 (19%); 41 (69%); HRCIMS m/z 397.1871 (C$_{20}$H$_{29}$O$_8$, calcd 397.1862). Unsaturation indexes: 6. The spectral data involving the LR & HRCIMS, 1D, 2D NMR (Fig. S85–S93†) and ECD (Fig. S94†) were inserted in the ESI data file.†

3.8. Tumor cell lines

In RPMI 1640 medium supplemented with 10% fetal bovine serum (FBS) and 1% penicillin (100 U mL^{-1})–streptomycin (100 µg mL^{-1}), CCRF-CEM leukaemia cells were grown. The MDA-MB-231-pcDNA3 and MCF-7 human breast cancer cell lines were grown in DMEM media with 10% FBS and 1% penicillin/streptomycin supplementation. All cell lines were maintained at 37 °C in a humid environment with 5% CO$_2$.

3.9. Resazurin cell viability assay

Living cells convert the inactive dye resazurin into the fluorescent dye resorufin through a metabolic process.[25] Suspension cells (1 × 10^4 cells per well) and/or adherent cells (5 × 10^3 cells per well, incubated for overnight to allow attachment) were seeded in 96-wells plate in a volume of 100 µL. Three cancer cell lines were screened using a single concentration (30 µm), and different concentrations of test substances were added to create a total volume of 200 µL for the creation of dose–response curves. After 72 h, 20 µL 0.01% w/v resazurin (Sigma-Aldrich) was added to each well. Cells were incubated for 4 h at 37 °C. Fluorescence at the excitation wavelength of 544 nm and emission at 590 nm was measured using Infinite M2000 Pro™ plate reader (Tecan, Crailsheim, Germany). Three independently performed assays for each set of six replicates were performed. Fifty percent inhibitory concentration (IC$_{50}$) values were calculated using the concentration–response curve fit to the non-linear regression model using GraphPad Prism® v8.0 software (GraphPad Software Inc., San Diego, CA, USA). All IC$_{50}$ values are expressed as mean ± standard deviation (SD). Previously, this protocol had been described.[26,27]

4. Conclusions

Ternifolipyrons A–J, ten new α-pyrone derivatives, and nine known metabolites have been isolated from the CH$_2$Cl$_2$–MeOH (1 : 1) extract of *I. ternifolius* roots. In addition to the ECD, X-ray signal crystal diffraction was used to determine the isolates' absolute stereochemistry. Ternifolipyron A, among of all isolated compounds, exhibited the most significant inhibitory effect on the growth of the MDA-MB-231 triple-negative breast cancer cell line, the MCF7 breast cancer cell line, and the CCRF-CEM leukaemia cell line.

Author contributions

Conflicts of interest

The authors declare no conflict of interest.

Acknowledgements

Notes and references

1 H.-D. Sun, S.-X. Huang and Q.-B. Han, *Nat. Prod. Rep.*, 2006, **23**, 673–698, DOI: 10.1039/b604174d.

2 Y. Zhang, K. Wang, H. Chen, R. He, R. Cai, J. Li, D. Zhou, W. Liu, X. Huang and R. Yang, *Phytochem*, 2018, **153**, 36–47, DOI: 10.1016/j.bmc.2020.115527.

3 X. Chen, X. Dai, Y. Liu, X. He and G. Gong, *Front. Pharmacol.*, 2022, **13**, 766581, DOI: 10.3389/fphar.2022.766581.

4 Y. Takeda and H. Otsuka, *Stud. Nat. Prod. Chem.*, 1995, **15**, 111–185, DOI: 10.1016/S1572-5995(06)80131-6.

5 M. Liu, W.-G. Wang, H.-D. Sun and J.-X. Pu, *Nat. Prod. Rep.*, 2017, **34**, 1090–1140, DOI: 10.1039/C7NP00027H.

6 J. Zou, X. Du, G. Pang, Y.-M. Shi, W.-G. Wang, R. Zhan, L.-M. Kong, X.-N. Li, Y. Li and J.-X. Pu, *Org. Lett.*, 2012, **14**, 3210–3213, DOI: 10.1021/ol3013205.

7 L.-L. Gou, K. Hu, Q. Yang, X.-N. Li, H.-D. Sun, C.-L. Xiang and P.-T. Puno, *Tetrahed*, 2019, **75**, 2797–2806, DOI: 10.1016/j.tet.2019.03.056.

8 H.-L. Zhang, Y. Zhang, X.-L. Yan, L.-G. Xiao, D.-X. Hu, Q. Yu and L.-K. An, *Bioorg. Med. Chem.*, 2020, **28**, 115527, DOI: 10.1016/j.bmc.2020.115527.

9 M. Q. Pham, T.-T.-H. Le, T.-L. Do, T.-H.-M. Pham, Q.-L. Pham, P.-H. Nguyen and D.-C. To, *Nat. Prod. Commun.*, 2020, **15**(9), 1–5, DOI: 10.1177/1934578X20953243.

10 M. Q. Pham, T. H. T. Le, T. T. Do, D. C. To, Q. L. Pham and N. P. Hung, *Vietnam J. Sci. Technol.*, 2020, **58**, 533–540, DOI: 10.15625/2525-2518/58/5/15012.

11 Y. J. Liao, H. Y. Bai, Z. H. Li, J. Zou, J. W. Chen, F. Zheng, J. X. Zhang, S. J. Mai, M. S. Zeng and H. D. Sun, *Cell Death Dis.*, 2014, **5**, e1137, DOI: 10.1038/cddis.2014.66.

12 R. Pereda-Miranda, M. García and G. Delgado, *Phytochem*, 1990, **29**, 2971–2974, DOI: 10.1016/0031-9422(90)87117-D.

13 L. A. Collett, M. T. Davies-Coleman and D. E. A. Rivett, *Phytochem*, 1998, **48**, 651–656, DOI: 10.1016/S0031-9422(97)01075-3.

14 J. A. Mendoza-Espinoza, F. López-Vallejo, M. Fragoso-Serrano, R. Pereda-Miranda and C. M. Cerda-Garcia-Rojas, *J. Nat. Prod.*, 2009, **72**, 700–708, DOI: 10.1021/np800447k.

15 J. García-Fortanet, J. Murga, M. Carda and J. A. Marco, *Tetrahed*, 2004, **60**, 12261–12267, DOI: 10.1016/j.tet.2004.10.010.

16 M. M. Rahman and S. Gibbons, *Fitoter*, 2015, **105**, 269–272, DOI: 10.1016/j.fitote.2015.07.012.

17 L. I. Li-Mei, P. U. Jian-Xin, X. Wei-Lie and S. U. N. Han-Dong, *Chin. J. Nat. Med.*, 2012, **10**, 307–310, DOI: 10.1016/S1875-5364(12)60063-6.

18 A. I. Elshamy, A.-R. H. Farrag, S. H. Mohamed, N. A. Ali, T. A. Mohamed, M. M. Menshawy, A. W. Zaglool, T. Efferth and M.-E. F. Hegazy, *Med. Chem. Res.*, 2020, **29**, 113–125, DOI: 10.1007/s00044-019-02465-8.

19 S. C. B. Gnoatto, A. Dassonville-Klimpt, S. Da Nascimento, P. Galéra, K. Boumediene, G. Gosmann, P. Sonnet and S. Moslemi, *Eur. J. Med. Chem.*, 2008, **43**, 1865–1877, DOI: 10.1016/j.ejmech.2007.11.021.

20 Z.-X. Hu, M. Liu, W.-G. Wang, X.-N. Li, K. Hu, X.-R. Li, X. Du, Y.-H. Zhang, P.-T. Puno and H.-D. Sun, *J. Nat. Prod.*, 2018, **81**, 106–116, DOI: 10.1021/acs.jnatprod.7b00723.

21 B. L. Li, Y. J. Pan, J. Li, L. Tong and K. B. Yu, *Cryst. Res. Technol.*, 2005, **40**, 810–814, DOI: 10.1002/crat.200410436.

22 W. Xiang, R.-T. Li, Z.-Y. Wang, S.-H. Li, Q.-S. Zhao, H.-J. Zhang and H.-D. Sun, *Phytochem*, 2004, **65**, 1173–1177, DOI: 10.1016/j.phytochem.2004.02.022.

23 N. D. Chaurasiya, V. Gogineni, K. M. Elokely, F. León, M. J. Núñez, M. L. Klein, L. A. Walker, S. J. Cutler and B. L. Tekwani, *J. Nat. Prod.*, 2016, **79**, 2538–2544, DOI: 10.1021/acs.jnatprod.6b00440.

24 D. H. Williams and I. Fleming, *Spectroscopic methods in organic chemistry*, Springer, London, 3rd end. 1980. p. 101.

25 J. O'Brien, I. Wilson, T. Orton and F. Pognan, *Eur. J. Biochem.*, 2000, **267**(16), 5421–5426, DOI: 10.1046/j.1432-1327.2000.01606.x.

26 M. Fukaya, S. Nakamura, M. E. F. Hegazy, Y. Sugimoto, N. Hayashi, S. Nakashima, M. Yoshikawa, T. Efferth and H. Matsuda, *Food Funct.*, 2018, **9**, 6279–6286, DOI: 10.1039/C8FO01804A.

27 M. E. F. Hegazy, S. Abdelfatah, A. R. Hamed, T. A. Mohamed, A. A. Elshamy, I. A. Saleh, E. H. Reda, N. S. Abdel-Azim, K. A. Shams, M. Sakr, Y. Sugimoto, P. W. Paré and T. Efferth, *Phytomed*, 2019, **59**, 152771, DOI: 10.1016/j.phymed.2018.11.031.